Electronic Supplementary Material (ESI) for Chemical Science.
This journal is © The Royal Society of Chemistry 2023

Supplementary Information

Critical assessment of selenourea as an efficient small molecule fluorescence quenching probe to monitor protein dynamics

Subhrakant Jena[a,b], Kiran Devi Tulsiyan[a,b,#], Rudhi Ranjan Sahoo[a,b,#], Saiprakash Rout[a,b], Akshay Kumar Sahu[a,b], and Himansu S. Biswal[a,b*]

[a]School of Chemical Sciences, National Institute of Science Education and Research (NISER), PO- Bhimpur-Padanpur, Via-Jatni, District- Khurda, PIN - 752050, Bhubaneswar, India

[b]Homi Bhabha National Institute, Training School Complex, Anushakti Nagar, Mumbai 400094, India

* Corresponding Author's E-mail: himansu@niser.ac.in and Phone No: - +91-674-2494 185/186

1. METHODS

Experimental section: Rhodamine 6G (Rh6G), phosphate buffer solution (PBS), urea, thiourea, selenourea, fluorescein free acid, and lysozyme were obtained from Sigma Aldrich. Urea and thiourea were recrystallized from diethyl ether solvent. The rest of the chemicals were used as received without further purification. The rhodamine 640, texas red 101, kitton red, rhodamine B, and coumarin 102 were purchased from Exciton dyes. Tetramethylrhodamine-5-malemide was purchased from Thermos-Fisher Scientific. Phosphate buffer solution (PBS) of 100 mM concentration was prepared using diluting a PBS solution of 1M. Rh6G and quencher solutions were prepared in PBS for steady-state absorption using 1mm and emission experiments using 2 mm path-length cuvettes. The TCSPC experiments were performed at similar fluorophore and quencher solution concentrations using 2 mm path cuvettes. Femtosecond time-resolved experiments were performed using 2mm path cuvettes.

Steady-state absorption experiments were recorded on a PerkinElmer LAMBDA 750 UV/VIS spectrophotometer. Steady-state fluorescence measurements were carried out using an Edinburgh FS5 spectrofluorometer. The time-resolved experiments were performed using a femtosecond fluorescence upconversion instrument (FluoMax from IB Photonics Ltd.) and a Ti-sapphire laser (Mai Tai HP, Spectra-Physics) centered at 800 nm and time-correlated single photon counting (TCSPC) techniques. Long lifetimes were measured with the help of an Edinburgh made OB920 TCSPC instrument considering 405 nm as the excitation source (diode laser, IRF of ~85 ps) using a 2 mm cuvette. Short lifetimes were measured using the femtosecond upconversion technique. The second harmonic of 800 nm fundamental ~400 nm was used for sample excitation (IRF ~300 ps), while the lifetimes were recorded at 550 nm. More details of this setup can be found elsewhere.[1] All the femtosecond time-resolved experiments were performed using 2mm cuvettes.

Fluorescence correlation spectroscopy (FCS) experiments were performed using a time-resolved confocal microscope (MicroTime 200, Picoquant). A pulsed diode laser of 483 nm was used as the excitation source. The excitation light source was focused onto the sample using a water immersion objective, and the fluorescence was collected through the same objective and passed through a long-pass dichroic mirror and a 485 nm long-pass filter. The light was allowed to pass through a 50 μm pinhole to filter out the stray signals and 50/50 beam splitter after-pulse contribution in the FCS curve before entering the two single-photon avalanche diodes (SPADs). The correlation curves were obtained by cross-correlating the

signal from two detectors and analyzed using SymphoTime software provided by PicoQuant. The experimental recordings use a laser power of 25 µW in a 100 mM PBS containing fluorophores in the nM concentration range. The equation for simple diffusion along with intersystem crossing is as follows:

$$G(\tau) = \frac{1-T+Te^{-\tau/\tau_{tr}}}{N(1-T)}\left(1+\frac{\tau}{\tau_D}\right)^{-1}\left(1+\frac{\tau}{\kappa^2\tau_D}\right)^{-1/2}$$

Here, τ is the correlation time, τ_D is the diffusion time, τ_{tr} is the triplet state lifetime, N represents the number of molecules in the observation volume, T is the fraction of molecules in the triplet state, and κ is the structure parameter defined as $\kappa = (\omega_z/\omega_{xy})$ in which ω_{xy} and ω_z are the transverse and longitudinal radii of the observation volume, respectively.[2, 3]

Computational section: Quantum chemical methods were used to study the electronic structure and relaxation processes of Urea, Thiourea, Selenourea, and Rh6G. All computations were performed using the Gaussian16 program.[4] The ground state (S_0) geometry optimization was performed using density functional theory (DFT) at the B3LYP/6-311++G(d,p) level of theory. The vertical excitation energies were calculated using time-dependent density functional theory (TD-DFT) at the PBE0/6-311++G (d,p) level of theory. All the calculations use the explicit integral equation formalism version of the polarizable continuum model (IEF-PCM) solvent model, considering water as the solvent. The natural bond orbital (NBO) and molecular electrostatic potential (MESP) calculations were done at the MP2/aug-cc-pVDZ level of theory. Molecular orbitals (MOs) analysis was performed to characterize and visualize the nature of the compounds. The MESP and MOs were visualized using the GaussView6 program. The NBO visualization was done using Chemcraft software.

2. Comparison of the structural properties of U, TU, and SeU.

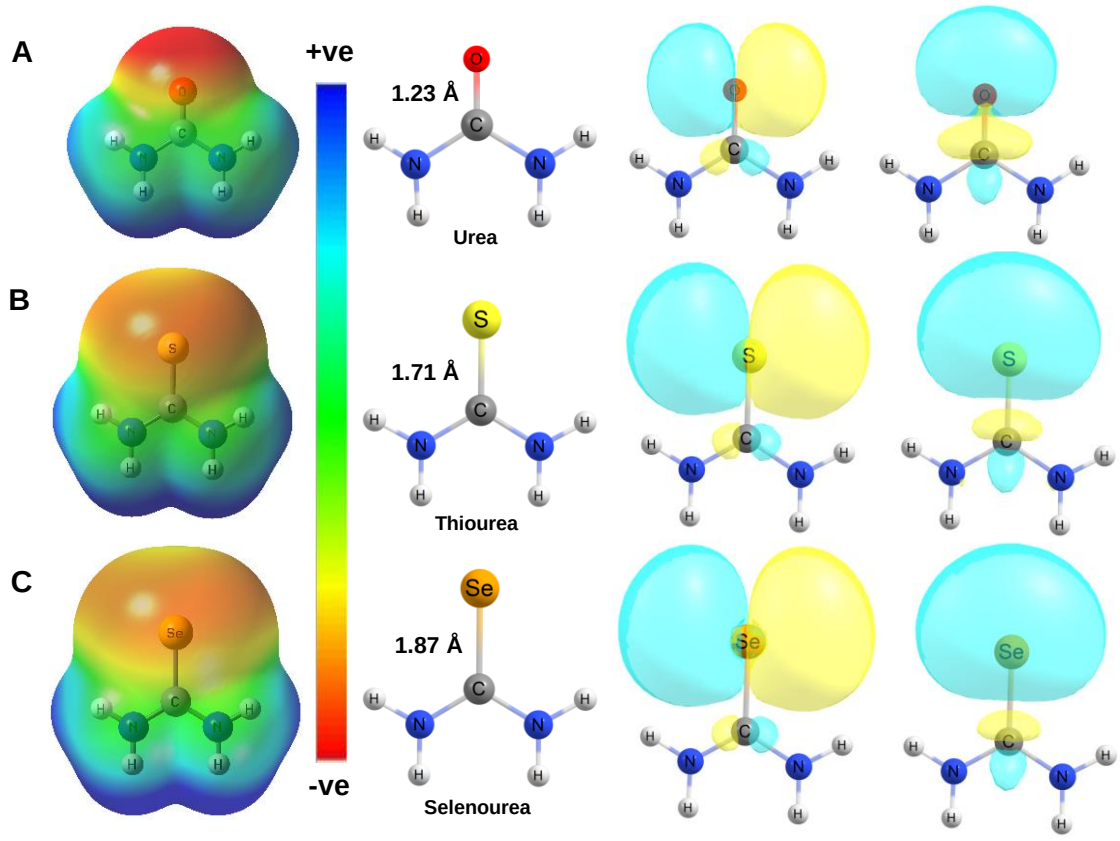

Figure S1. Molecular structures, visualization of molecular electrostatic potential (MESP, isovalue = 0.005), the Natural Bond Orbitals (NBO, isovalue = 0.02) showing diffused lone pair electron visualization from NBO calculation of (A) Urea (U); (B) Thiourea (TU); (C) Selenourea (SeU). The MESP and NBO calculations were performed at the MP2/aug-cc-pVDZ level of theory.

3. Equations used for the calculation of photophysical parameters.

$$E_Q(SS) = 1 - \frac{F}{F_0} \qquad (Eq.\ S1)$$

$$E_Q(\tau) = 1 - \frac{\tau}{\tau_0} \qquad (Eq.\ S2)$$

$$\frac{F_0}{F} = \frac{\tau_0}{\tau} = 1 + K_{SV}\,[Q] \qquad (Eq.\ S3)$$

$$\frac{F_0}{F} = (1 + K_S[Q])(1 + K_D[Q]) \qquad (Eq.\ S4)$$

$$\frac{F_0}{F} = (1 + K_{SV}\,[Q])\exp(V[Q]) \qquad (Eq.\ S5)$$

$$K_{SV} = K_Q \times \tau_0 \qquad (Eq.\ S6)$$

$$K_2 = \frac{2RT}{3\eta}\left(\frac{\left(R_F + R_Q\right)^2}{R_F R_Q}\right)(1000) \qquad (Eq.\ S7)$$

$$f_Q = \frac{K_Q}{K_2} \qquad (Eq.\ S8)$$

4. Fluorescence titration for Rh6G-Urea donor-acceptor pair.

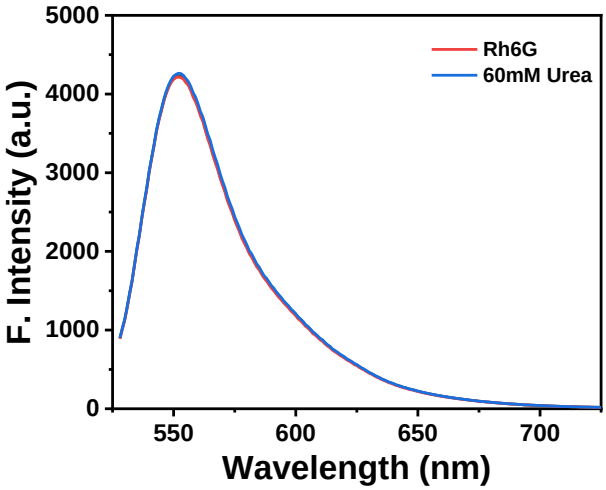

Figure S2. Spectra showing no quenching in the Rh6G fluorescence upon addition 60mM urea.

5. Steady-state absorption studies of Rh6G in the presence of quenchers.

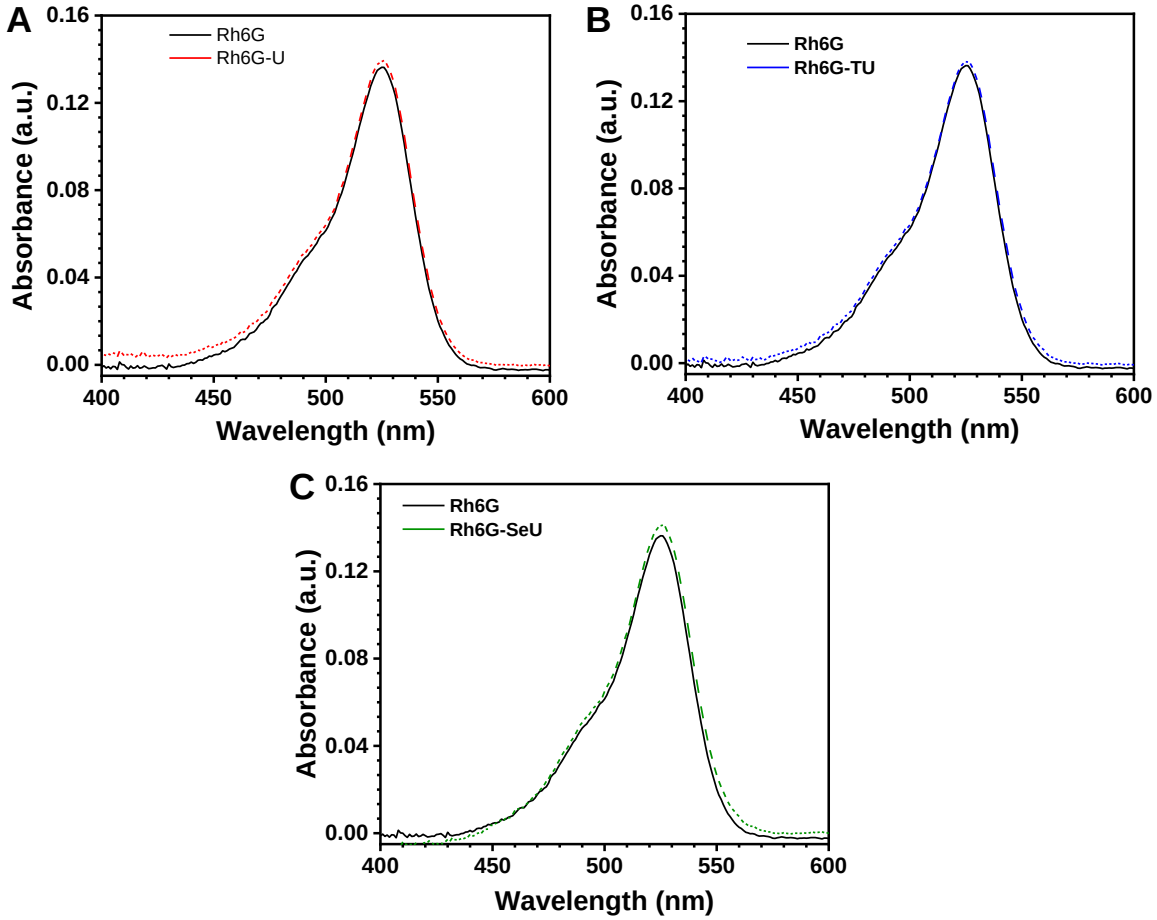

Figure S3. Steady-state spectra showing no change in the Rh6G absorbance upon the addition of 60 mM (A) urea (U);(B) Thiourea (TU); (C) Selenourea (SeU).

6. Temperature-dependent lifetime measurements for Rh6G-TU pair.

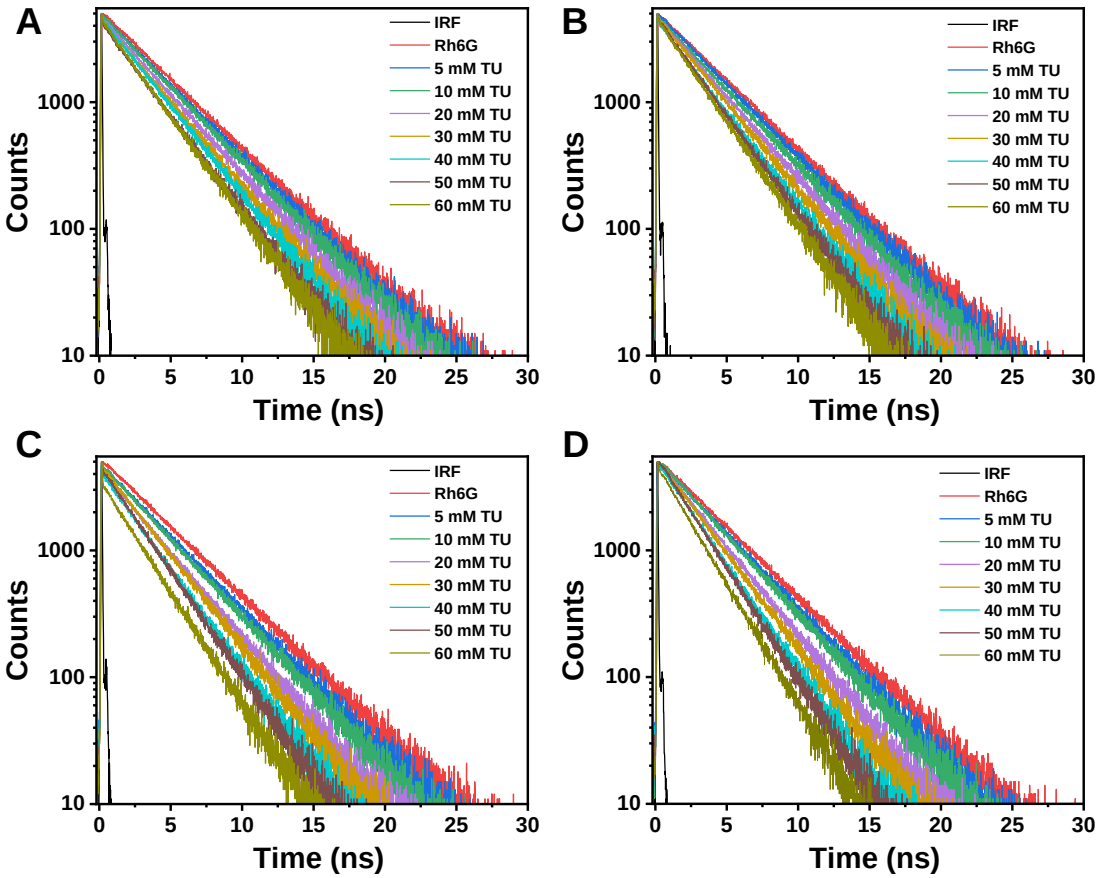

Figure S4. Temperature dependent fluorescence lifetime titration studies for the Rh6G-TU pair at (A) 10° C; (B) 25° C; (C) 40° C (D) 60° C.

7. Table S1. Single exponential fitted lifetime values for the temperature-dependent studies for Rh6G-TU donor-acceptor pair.

TU Concentration (mM)	**10°** C **Lifetime (ns)**	**25°** C **Lifetime (ns)**	**40°** C **Lifetime (ns)**	**60°** C **Lifetime (ns)**
0	3.93	3.94	3.93	3.9
5	3.78	3.77	3.73	3.65
10	3.65	3.63	3.55	3.46
20	3.44	3.37	3.24	3.11
30	3.25	3.14	2.99	2.84
40	3.06	2.94	2.79	2.61
50	2.9	2.75	2.6	2.43
60	2.77	2.62	2.45	2.26

8. Temperature-dependent lifetime measurement for Rh6G-SeU pair.

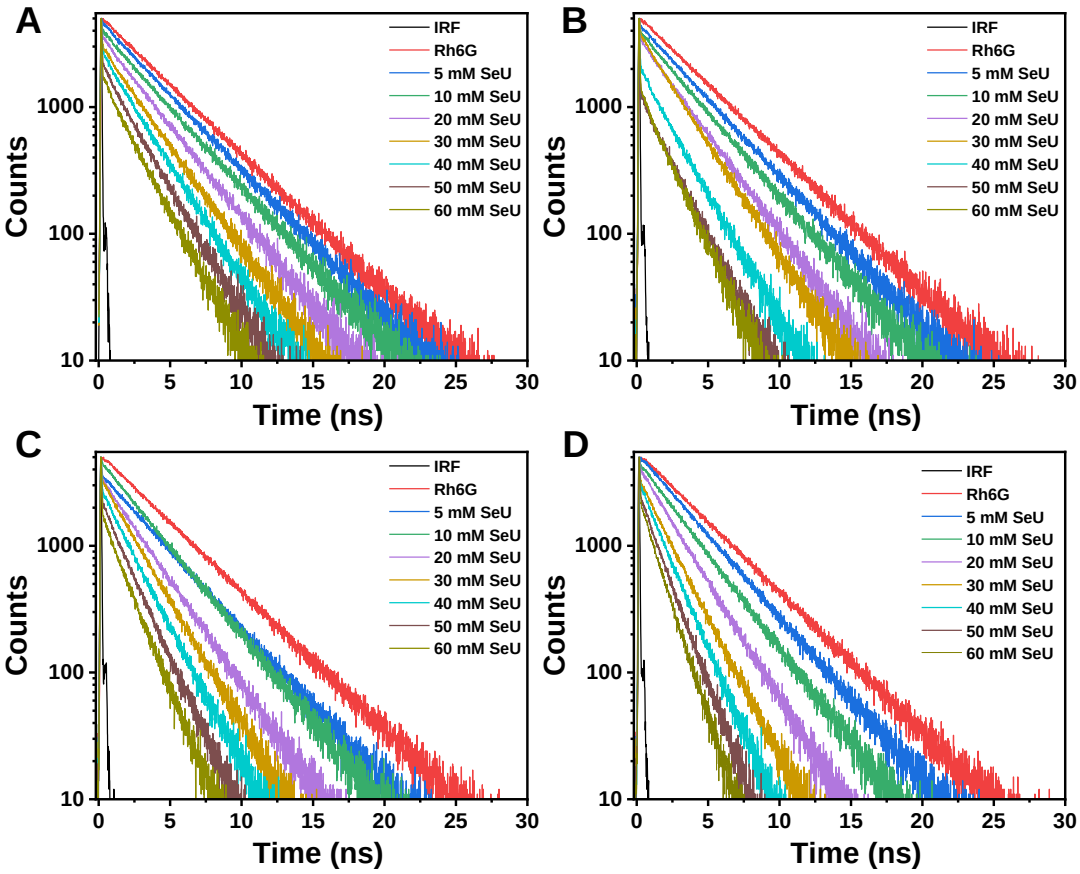

Figure S5. Temperature-dependent fluorescence lifetime titration studies for the Rh6G-SeU pair at (A) 10° C; (B) 25° C; (C) 40° C (D) 60° C.

9. Table S2. Single exponential fitted lifetime values for the temperature-dependent studies for Rh6G-SeU donor-acceptor pair.

SeU Concentration (mM)	10° C	25° C	40° C	60° C
	Lifetime (ns)	**Lifetime (ns)**	**Lifetime (ns)**	**Lifetime (ns)**
0	3.93	3.94	3.93	3.9
5	3.65	3.56	3.48	3.32
10	3.42	3.26	3.08	2.89
20	2.99	2.77	2.6	2.32
30	2.66	2.42	2.19	1.93
40	2.37	2.1	1.94	1.6
50	2.14	1.89	1.7	1.4
60	1.94	1.69	1.51	1.22

10. Stern-Volmer plots generated from temperature-dependent TCSPC experiments.

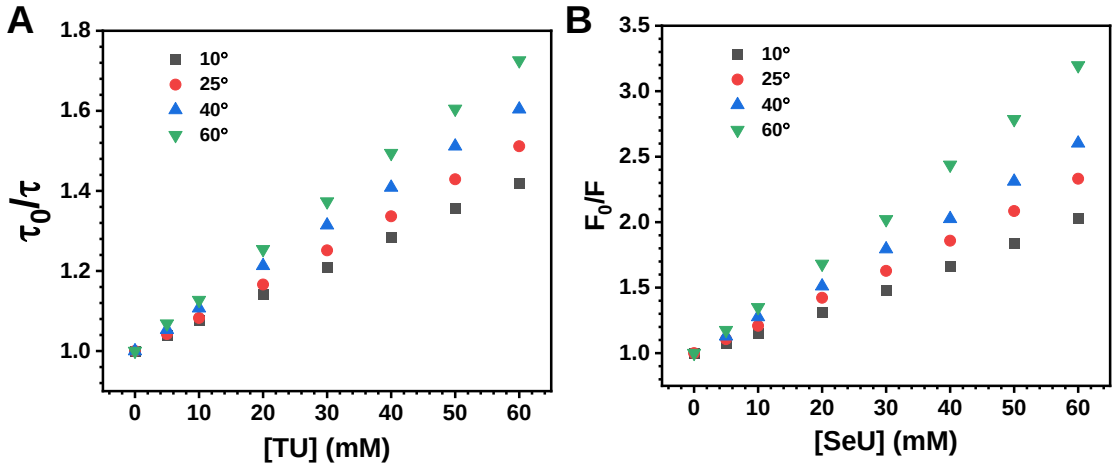

Figure S6. Comparison of Stern-Volmer plots with the increase in the temperature from 10° to 60°C; (A) Rh6G-TU; (B) Rh6G-SeU.

11. Femtosecond fluorescence transients.

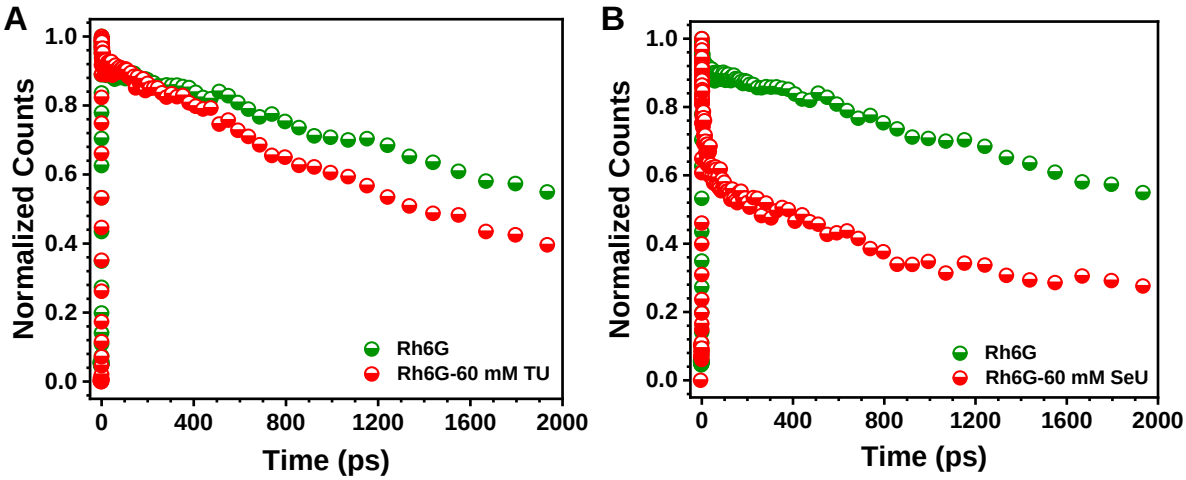

Figure S7. (A) Normalized femtosecond transients of Rh6G in the absence (green) and presence of 60 mM TU (red); (B) Normalized femtosecond transients of Rh6G in the absence (green) and presence of 60mM SeU (red).

12. Table S3. Quenching studies for the selected fluorophores and the comparison of their photo physical properties in the presence of TU and SeU. *Error Estimates: ± 1% for TU and ± 3% for SeU.*

F-Q pairs	**$\lambda_{ex}/\lambda_{em}$ (nm)**	**E_Q (SS) [%]**	**τ (ns)**	**E_Q (τ) [%]**	**E_Q (Static) [%]**
C102	390/490		5.84		
C102-TU	390/490	0	5.85	0	0
C102-SeU	390/490	60	3.97	32	28
Fluorescein	487/516		4.14		
Fluorescein-TU	487/516	48	2.19	48	0
Fluorescein-SeU	487/516	58	1.92	54	4
Rh6G	526/554		3.95		
Rh6G-TU	526/554	34	2.61	33	1
Rh6G-SeU	526/554	74	1.73	58	16
TMR	552/574		2.16		
TMR-TU	552/574	13	1.89	13	0
TMR-SeU	552/574	53	1.32	39	14
RhB	554/578		1.56		
RhB-TU	554/578	6	1.50	4	2
RhB-SeU	554/578	43	1.09	29	14
Kitton Red	566/585		1.66		
Kitton Red-TU	566/585	0	1.64	0	0
Kitton Red-SeU	566/585	47	1.13	33	14
Rh640	576/599		4.27		
Rh640-TU	576/599	0	4.28	0	0
Rh640-SeU	576/599	52	2.39	45	7
Texas Red	587/607		4.27		
Texas Red-TU	587/607	0	4.25	0	0
Texas Red-SeU	587/607	52	2.48	42	10
Lys-TMR	552/576		2.47		
Lys-TMR-TU	552/576	28	2.09	15	13
Lys-TMR-SeU	552/576	60	1.47	40	20

13. Quenching studies of Fluorescein free acid.

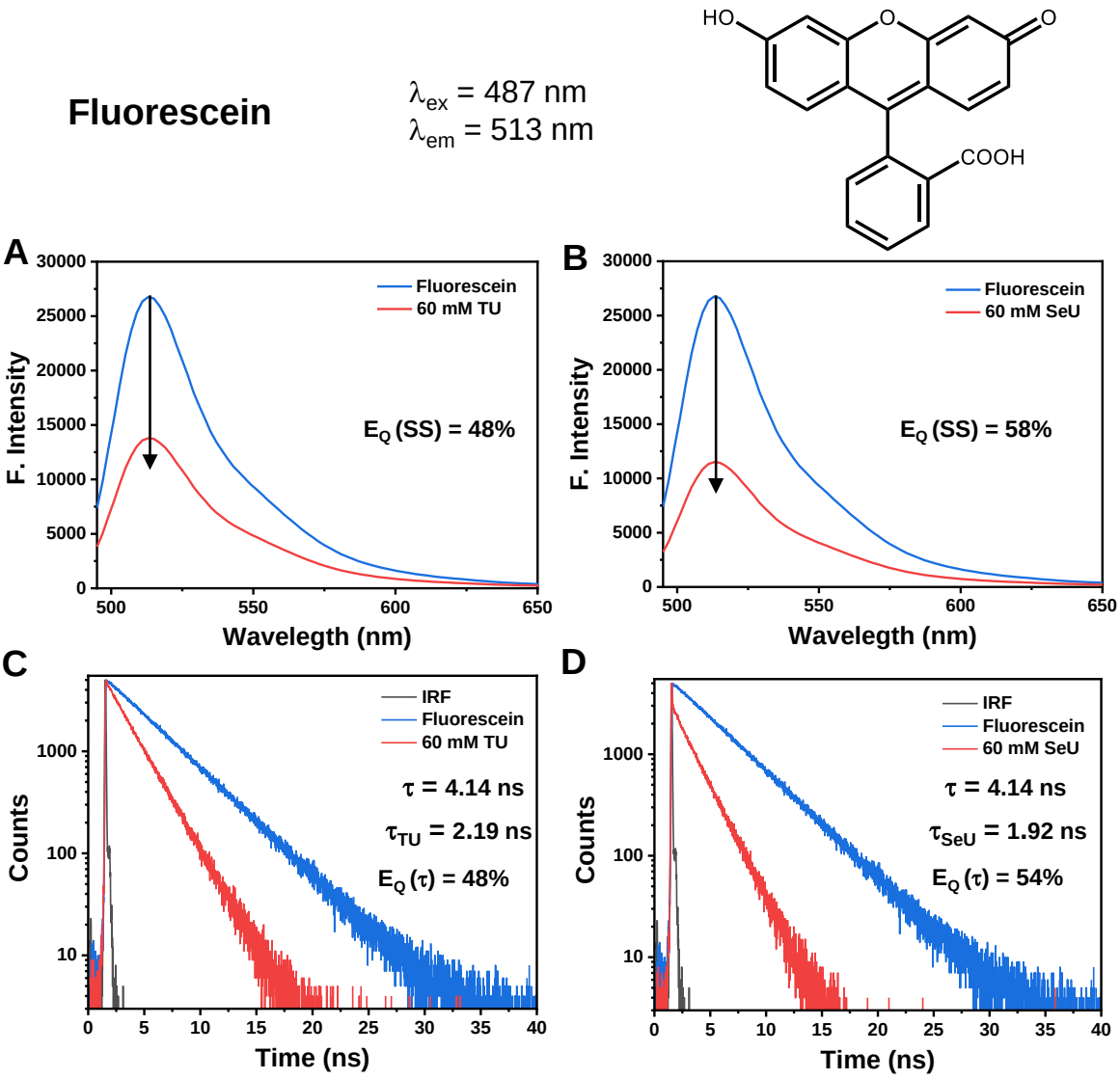

Figure S8. Molecular structure of fluorescein and the observation from quenching experiments carried out in 100 mM phosphate buffer solution of PH 7.4. Fluorescein concentration is 3 μM calculated from ε_{490} = 70,000 $M^{-1}cm^{-1}$. Steady-state (SS) fluorescence spectra of fluorescein excited at 487 nm in the presence of A) 60 mM TU; B) 60 mM SeU. Time-resolved (TR) lifetime decay profiles of fluorescein excited at 405 nm and collected emission at 513 nm in the presence of A) 60 mM TU; B) 60 mM SeU. The quenching efficiency obtained from SS and TR due to the photo-induced electron transfer process is also shown. The lifetime values are obtained from a single exponential fit. The presence of an ultra-short component within the IRF region in the case of SeU is avoided during fitting.

14. Quenching studies of Rhodamine 640.

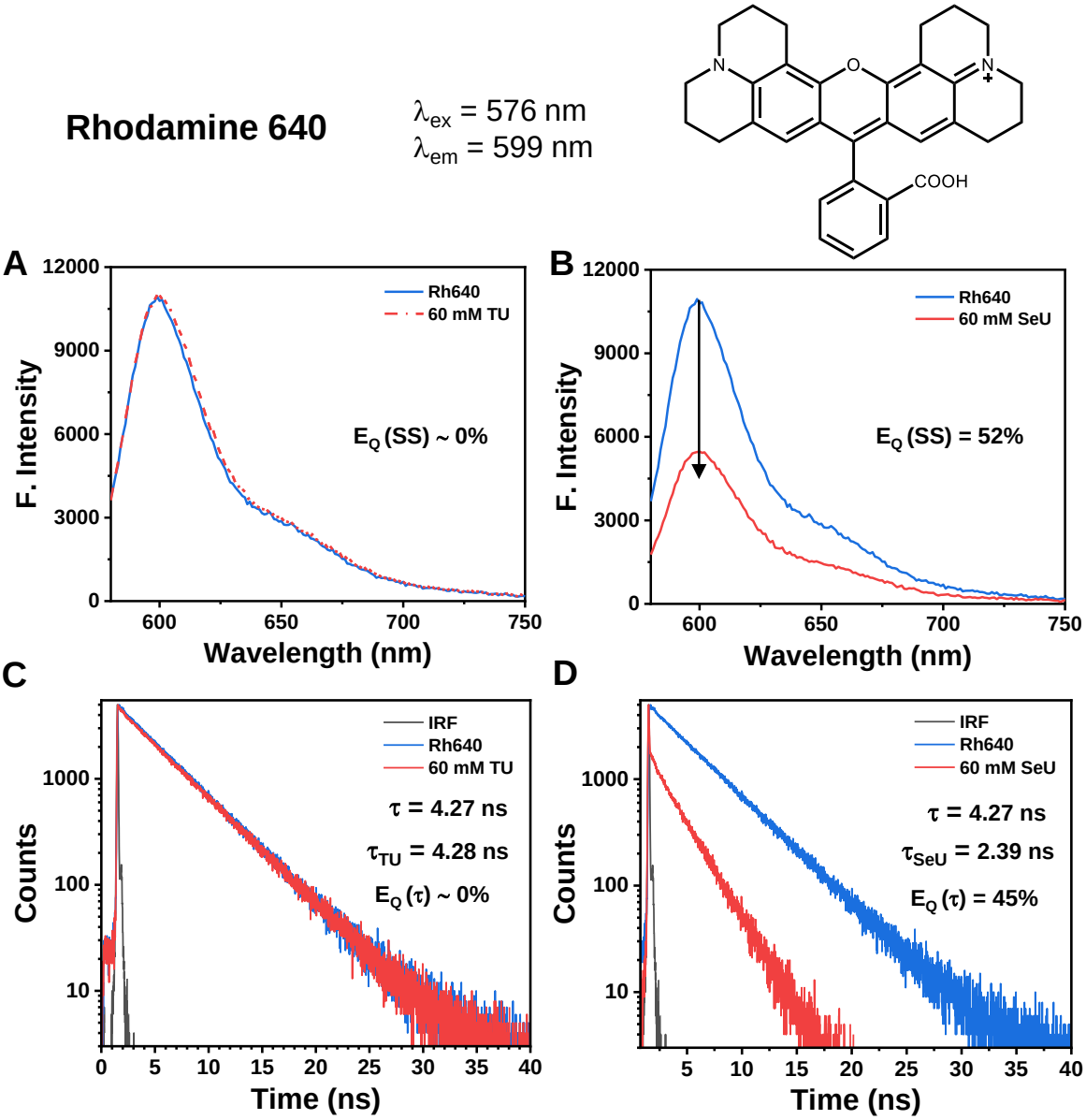

Figure S9. Molecular structure of Rhodamine 640 (Rh 640) and the observation from quenching experiments carried out in 100 mM phosphate buffer solution of PH 7.4. Rh 640 concentration is 2 μM calculated from ε_{567} = 105,000 $M^{-1}cm^{-1}$. Steady-state (SS) fluorescence spectra of Rhodamine 640 excited at 576 nm in presence A) 60 mM TU; B) 60 mM SeU. Time-resolved (TR) lifetime decay profiles of fluorescein excited at 405 nm and collected emission at 599 nm in the presence of A) 60 mM TU; B) 60 mM SeU. The quenching efficiency obtained from SS and TR due to the photo-induced electron transfer process is also shown. The lifetime values are obtained from a single exponential fit. The presence of an ultra-short component within the IRF region in the case of SeU is avoided during fitting.

15. Quenching studies of Texas Red.

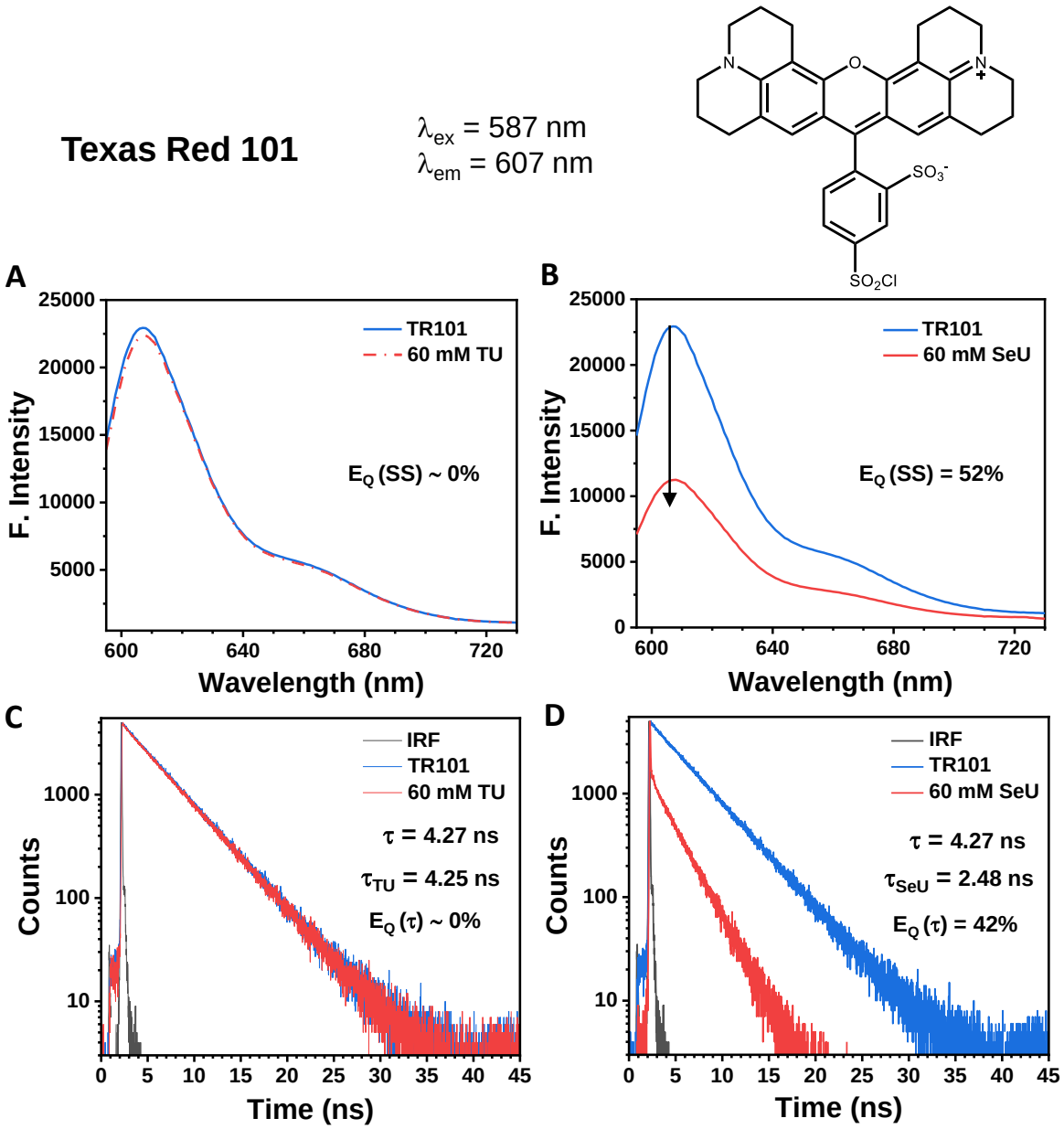

Figure S10. Molecular structure of Texas Red 101 (TR 101) and the observation from quenching experiments carried out in 100 mM phosphate buffer solution of PH 7.4. TR 101 concentration is 2 μM calculated from ε_{578} = 139,000 $M^{-1}cm^{-1}$. Steady-state (SS) fluorescence spectra of TR 101 excited at 587 nm in presence A) 60 mM TU; B) 60 mM SeU. Time-resolved (TR) lifetime decay profiles of TR 101 excited at 405 nm and collected emission at 607 nm in the presence of A) 60 mM TU; B) 60 mM SeU. The quenching efficiency obtained from SS and TR due to the photo-induced electron transfer process is also shown. The lifetime values are obtained from a single exponential fit. The presence of an ultra-short component within the IRF region in the case of SeU is avoided during fitting.

16. Quenching studies of Kitton Red.

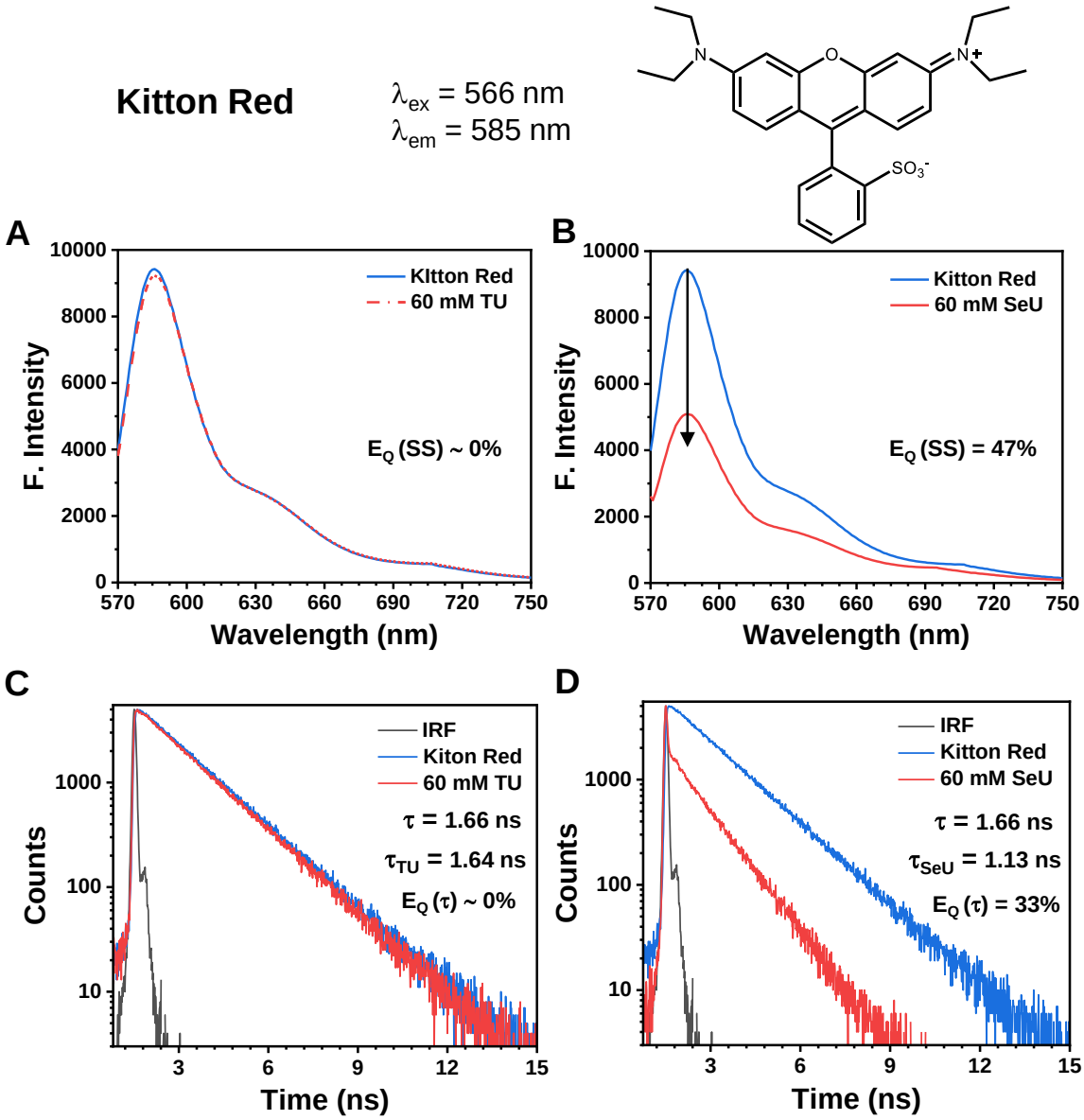

Figure S11. Molecular structure of Kitton Red and the observation from quenching experiments carried out in 100 mM phosphate buffer solution of PH 7.4. Kitton red concentration is 2 μM calculated from ε_{578} = 118,000 $M^{-1}cm^{-1}$. Steady-state (SS) fluorescence spectra of Kitton Red excited at 566 nm in presence A) 60 mM TU; B) 60 mM SeU. Time-resolved (TR) lifetime decay profiles of Kitton Red excited at 405 nm and collected emission at 585 nm in the presence of A) 60 mM TU; B) 60 mM SeU. The quenching efficiency obtained from SS and TR due to the photo-induced electron transfer process is also shown. The lifetime values are obtained from a single exponential fit. The presence of an ultra-short component within the IRF region in the case of SeU is avoided during fitting.

17. Quenching studies of Coumarin 102 (C102).

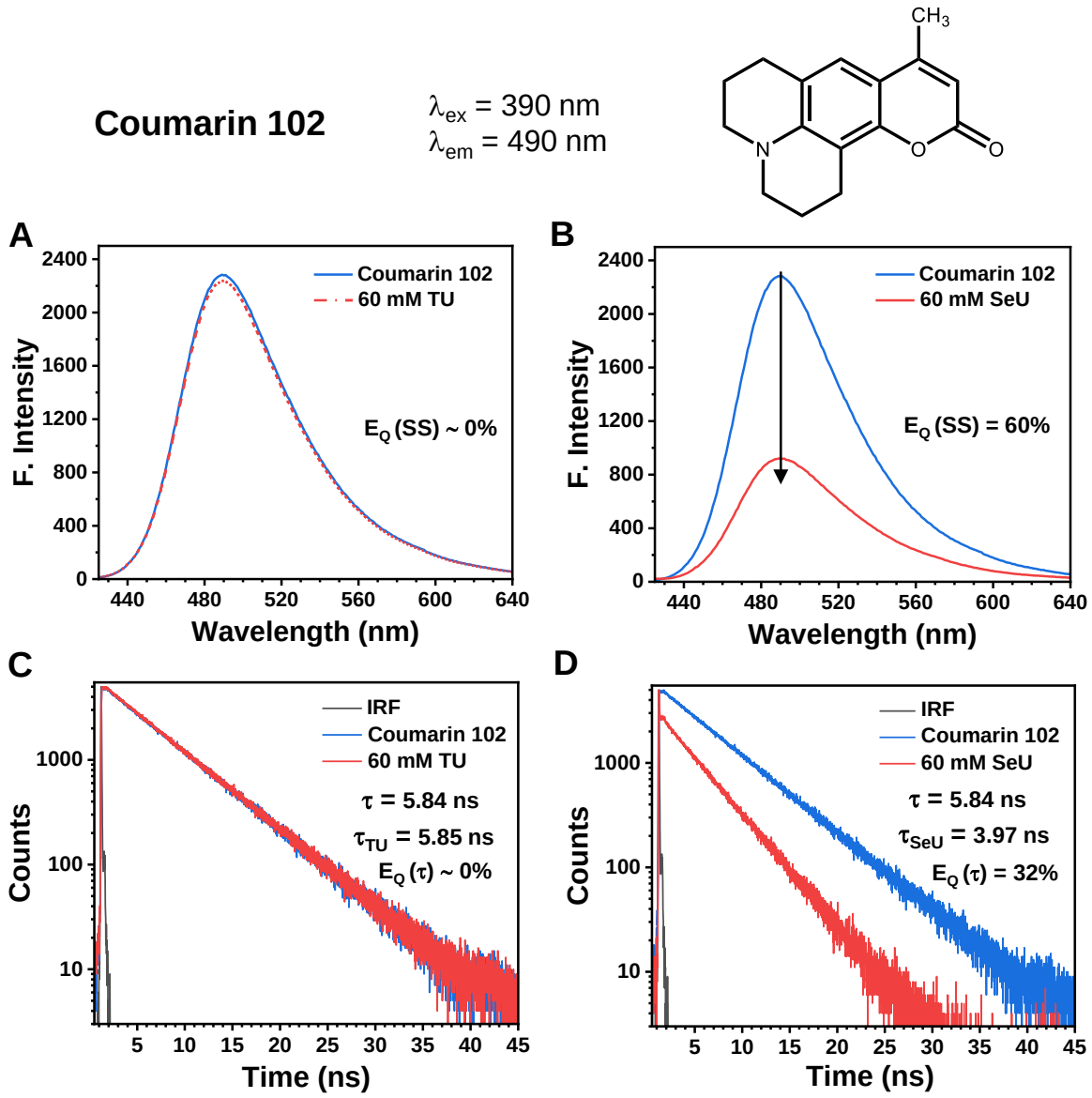

Figure S12. Molecular structure of C102 and the observation from quenching experiments carried out in 100 mM phosphate buffer solution of PH 7.4. C102 concentration is 2 μM calculated from ε_{387} = 23,000 $M^{-1}cm^{-1}$. Steady-state (SS) fluorescence spectra of C102 excited at 390 nm in presence A) 60 mM TU; B) 60 mM SeU. Time-resolved (TR) lifetime decay profiles of C102 excited at 405 nm and collected emission at 490 nm in the presence of A) 60 mM TU; B) 60 mM SeU. The quenching efficiency obtained from SS and TR due to the photo-induced electron transfer process is also shown. The lifetime values are obtained from a single exponential fit. The presence of an ultra-short component within the IRF region in the case of SeU is avoided during fitting.

18. Quenching studies of Rhodamine B (RhB).

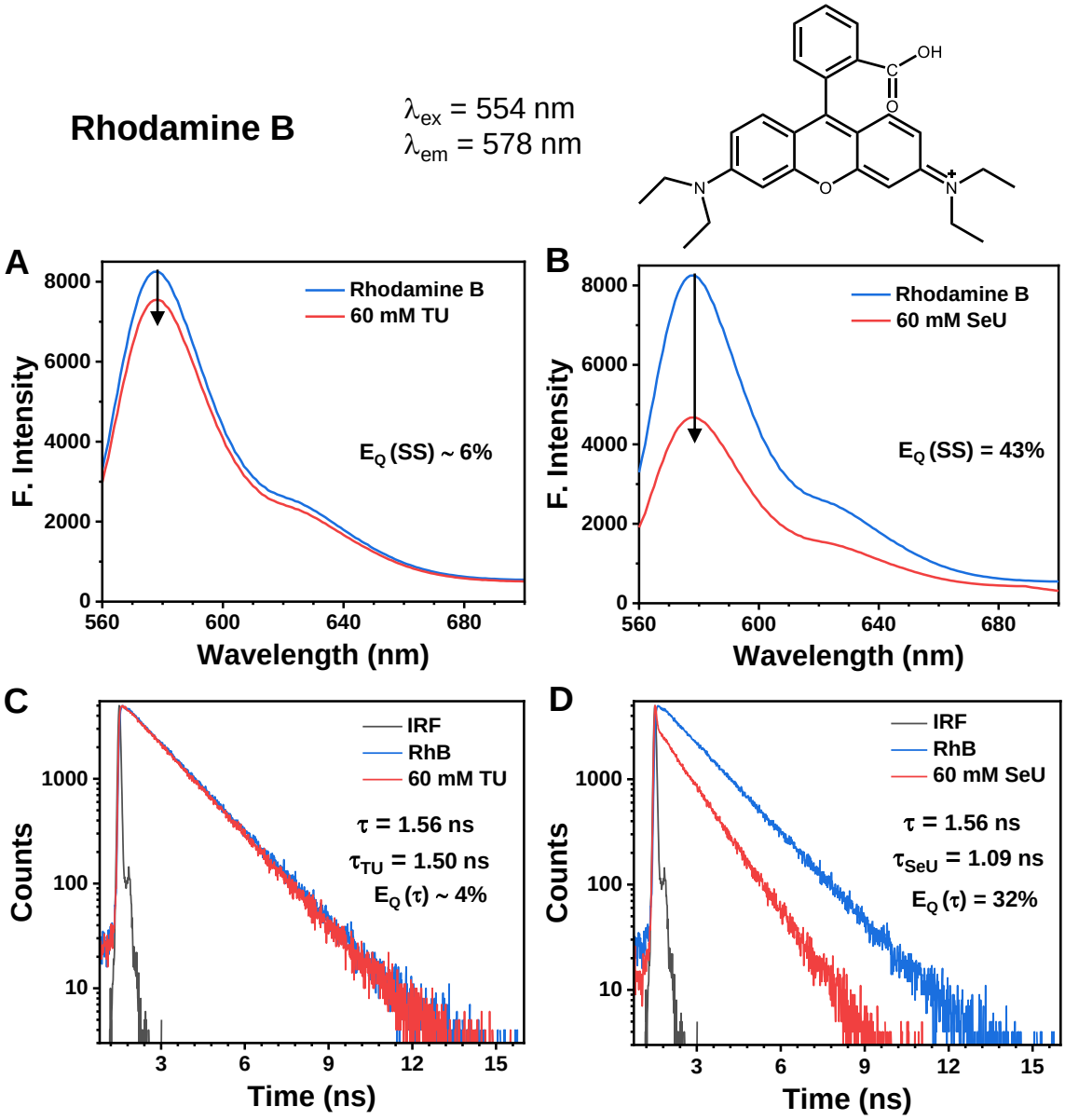

Figure S13. Molecular structure of Rhodamine B and the observation from quenching experiments carried out in 100 mM phosphate buffer solution of PH 7.4. Rhodamine B concentration is 2 μM calculated from ε_{555} = 106,000 $M^{-1}cm^{-1}$. Steady-state (SS) fluorescence spectra of Rhodamine B excited at 554 nm in presence A) 60 mM TU; B) 60 mM SeU. Time-resolved (TR) lifetime decay profiles of Rhodamine B excited at 405 nm and collected emission at 578 nm in the presence of A) 60 mM TU; B) 60 mM SeU. The quenching efficiency obtained from SS and TR due to the photo-induced electron transfer process is also shown. The lifetime values are obtained from a single exponential fit. The presence of an ultra-short component within the IRF region in the case of SeU is avoided during fitting.

19. Lysozyme labeling experiments: The labeling of tetramethylrhodamine-5-malemide (TMR-5-Malemide, provided by Thermo Fisher Scientific) to lysozyme was carried out according to the methodology provided by the manufacturer and previously reported literature.[5, 6] It is a thiol-reactive dye and yields pH sensitive photostable fluorescent conjugates with biomolecules. This dye reacts with the cysteine groups present in lysozyme protein and covalently binds to it. The protein concentration was kept at 60 μM (3 ml), and the dye concentration in DMSO was at 1mM (500 μl). The labeling reaction was allowed to proceed for 2 hrs at room temperature using 100 mM PBS with the help of a 3D-shaker.

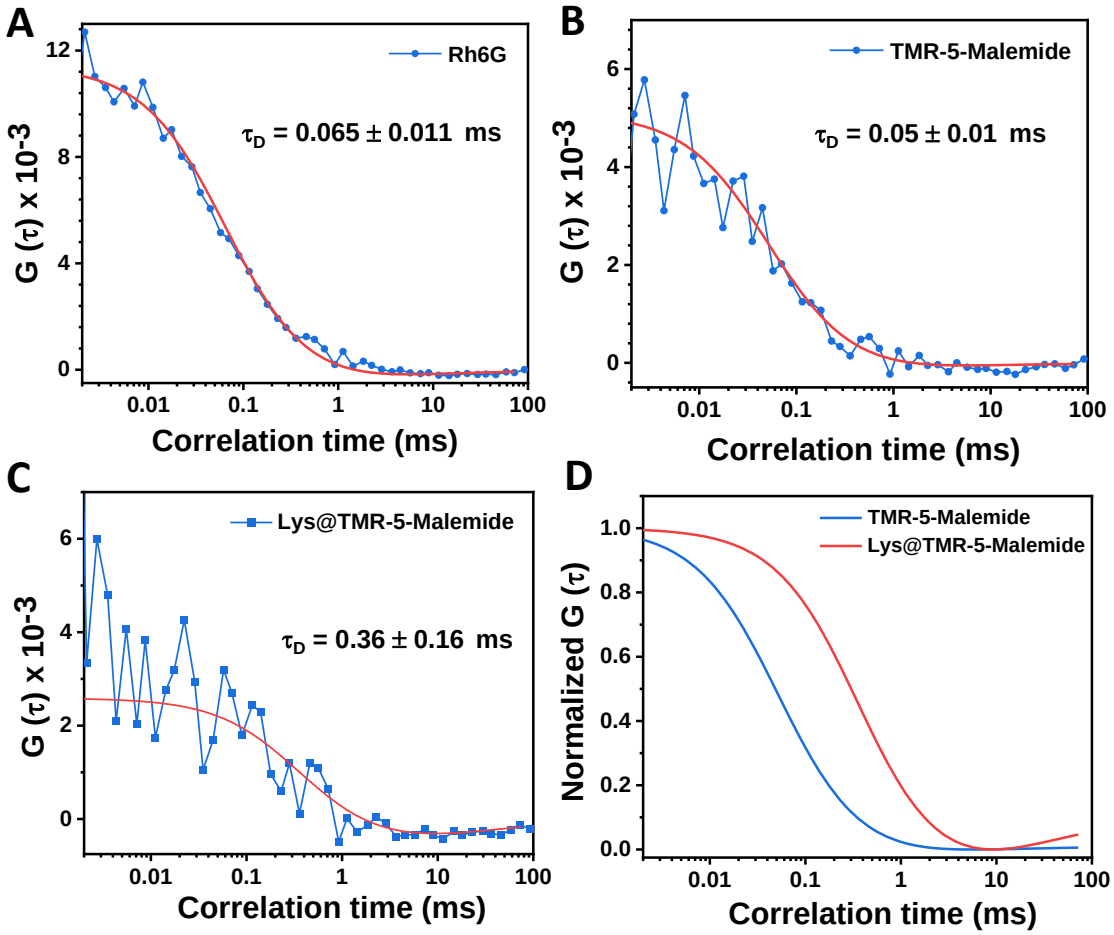

Figure S14. Autocorrelation function obtained from FCS studies of A) Rhodamine 6G (Rh6G); B) TMR-5-Malemide; C) TMR-5-Malemide labeled lysozyme; D) Comparison between normalized autocorrelation function of TMR-5-Malemide and its bound form. The concentrations of the studied fluorophores were in the ~ nM range. The curves were fitted using simple diffusion along with the intersystem crossing equation as described in the details of the FCS study. The instrument was calibrated using Rh6G as the reference.

The unreacted free dye was removed from the mixture using Sephadex G-25 column chromatography equilibrated in PBS. The dye concentration in the labeled protein was

calculated from the reported ε_{552} = 90,000 $M^{-1}cm^{-1}$. The labeling was further confirmed using FCS studies, as shown in Figure S14.

20. Quenching studies of Tetramethylrhodamine (TMR)-5-malemide.

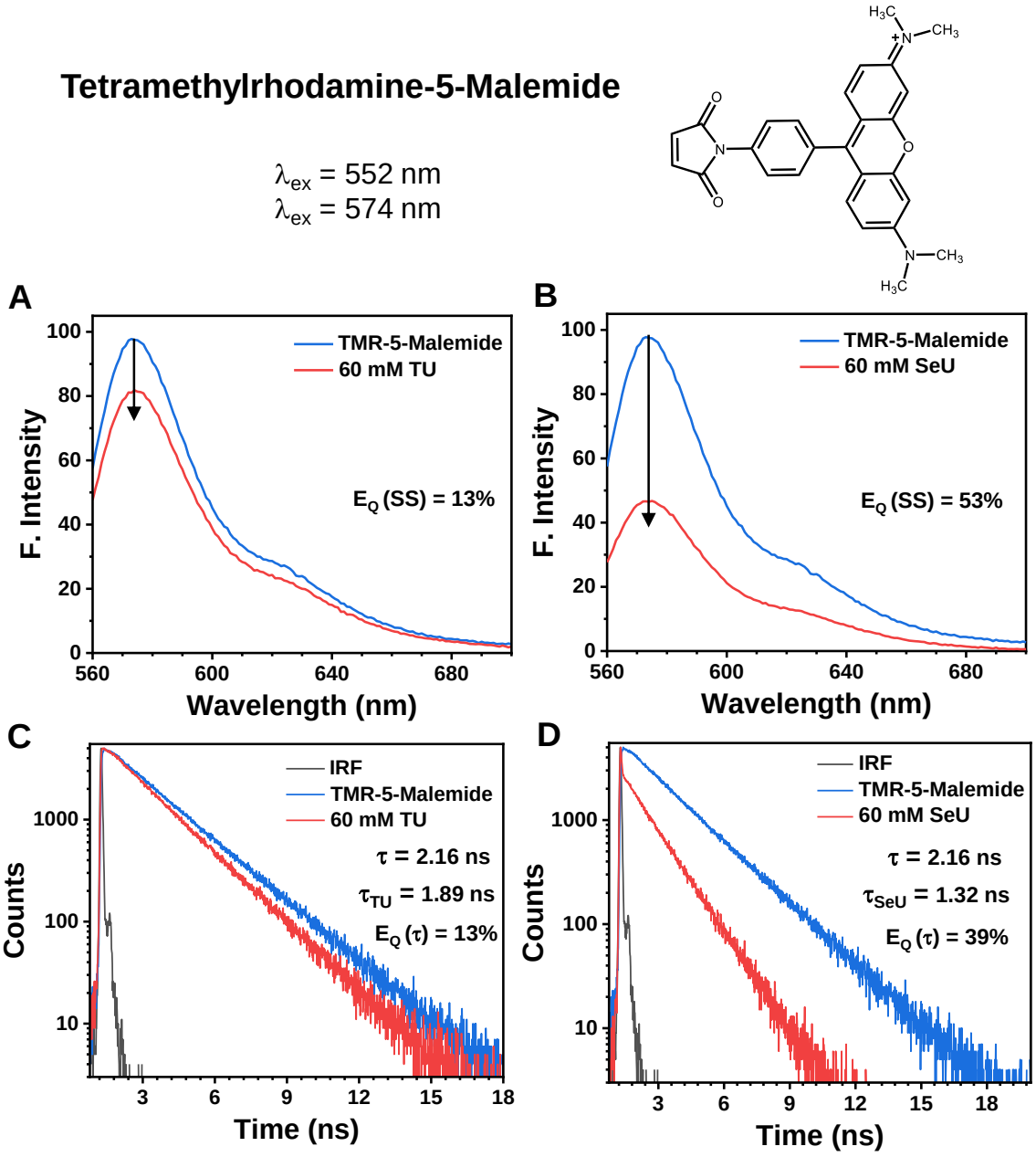

Figure S15. Molecular structure of TMR-5-malemide and the observation from quenching experiments carried out in 100 mM phosphate buffer solution of PH 7.4. TMR-5-Malemide concentration is 1 μM calculated from ε_{552} = 90,000 $M^{-1}cm^{-1}$. Steady-state (SS) fluorescence spectra of TMR-5-Malemide excited at 552 nm in presence A) 60 mM TU; B) 60 mM SeU. Time-resolved (TR) lifetime decay profiles of TMR-5-Malemide excited at 405 nm and collected emission at 574 nm in the presence of A) 60 mM TU; B) 60 mM SeU. The quenching

efficiency obtained from SS and TR due to the photo-induced electron transfer process is also shown. The lifetime values are obtained from a single exponential fit. The presence of an ultra-short component within the IRF region in the case of SeU is avoided during fitting.

21. Quenching studies of Tetramethylrhodamine (TMR)-5-malemide-Lysozyme.

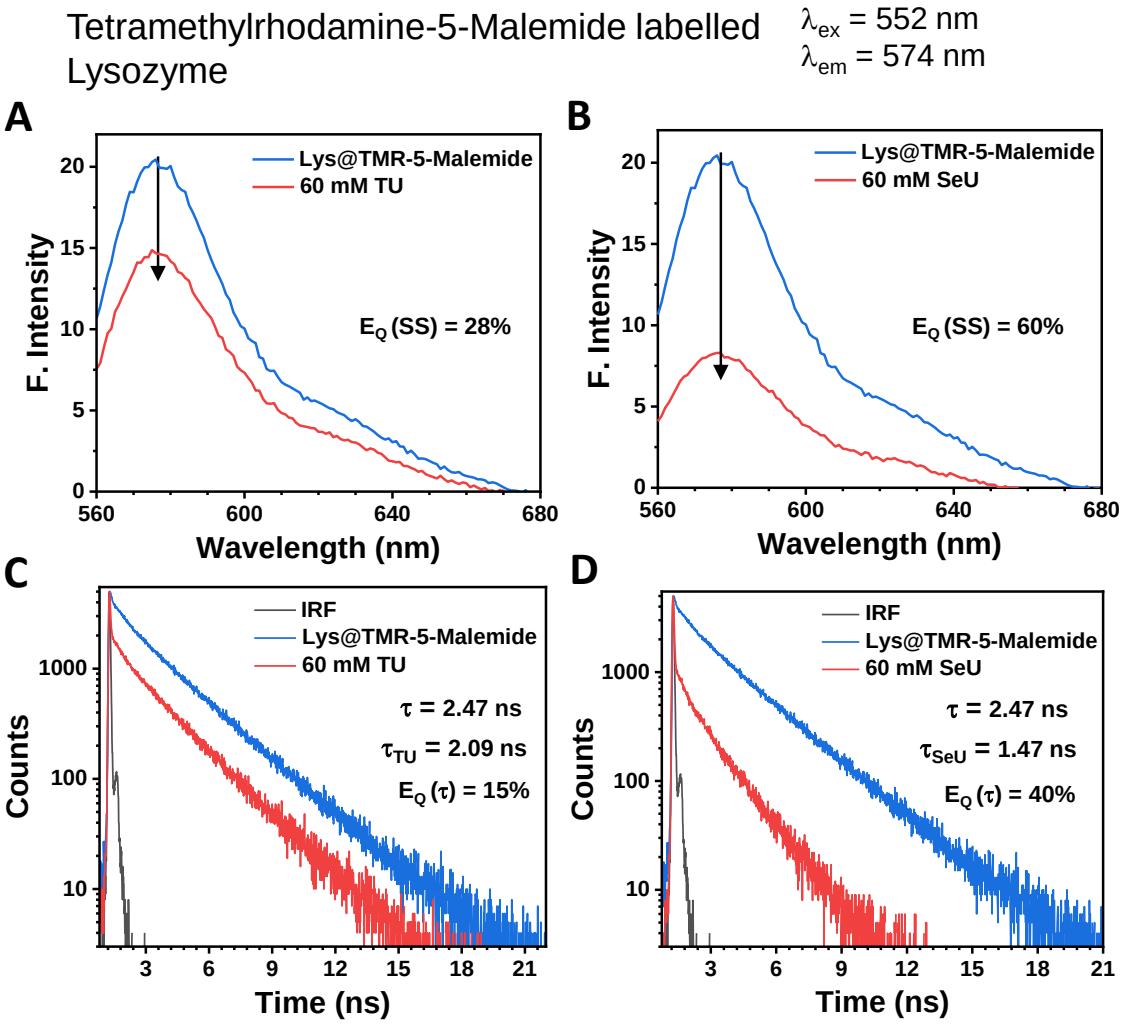

Figure S16. Observation from quenching experiments carried out in 100 mM phosphate buffer solution of PH 7.4. TMR-5-Malemide concentration in the labeled protein is 1 μM calculated from ε_{552} = 90,000 $M^{-1}cm^{-1}$. Steady-state (SS) fluorescence spectra of TMR-5-Malemide excited at 552 nm in presence A) 60 mM TU; B) 60 mM SeU. Time-resolved (TR) lifetime decay profiles of TMR-5-Malemide excited at 405 nm and collected emission at 574 nm in the presence of A) 60 mM TU; B) 60 mM SeU. The quenching efficiency obtained from SS and TR due to the photo-induced electron transfer process is also shown. The lifetime values are obtained from a single exponential fit. The presence of an ultra-short component within the IRF region is avoided during fitting.

22. Cartesian coordinates of the optimized geometries.

Rh6G, C1, imaginary frequency=0, E= -1421.1112901 a.u

O	-0.334457000	-2.144790000	0.349148000
C	-1.423106000	-1.362724000	0.123262000
C	-1.277085000	-0.048673000	-0.394043000
C	0.014523000	0.444489000	-0.657964000
C	1.126188000	-0.391365000	-0.442351000
C	0.919476000	-1.697150000	0.075210000
C	1.957108000	-2.570638000	0.322689000
C	3.284021000	-2.171695000	0.067241000
C	3.538115000	-0.849020000	-0.461848000
C	2.477644000	-0.016359000	-0.695029000
C	-2.652817000	-1.912610000	0.416973000
C	-3.824485000	-1.158125000	0.209775000
C	-3.720063000	0.183887000	-0.321149000
C	-2.479176000	0.688478000	-0.600363000
H	2.667796000	0.974210000	-1.089168000
H	1.724653000	-3.553241000	0.706882000
N	4.329945000	-2.988911000	0.316578000
H	-2.689256000	-2.922693000	0.798468000
H	-2.400829000	1.693111000	-0.997027000
N	-5.046306000	-1.651867000	0.505123000
C	0.195497000	1.796950000	-1.271376000
C	0.349220000	2.986527000	-0.529731000
C	0.508318000	4.202828000	-1.208672000
C	0.516909000	4.251470000	-2.597527000
C	0.364201000	3.076573000	-3.329625000
C	0.204919000	1.861190000	-2.668520000
H	0.085332000	0.948737000	-3.240706000

H	0.368632000	3.100852000	-4.413008000
H	0.642226000	5.200747000	-3.104288000
H	0.626926000	5.110870000	-0.634054000
C	0.347742000	2.952648000	0.965226000
O	0.260743000	1.934767000	1.623095000
O	0.447820000	4.176854000	1.502783000
C	0.471805000	4.286550000	2.956561000
H	0.047656000	5.270765000	3.150882000
H	-0.182877000	3.522220000	3.373691000
C	1.887171000	4.174322000	3.493829000
H	2.534141000	4.934299000	3.050013000
H	2.310430000	3.188006000	3.294636000
H	1.872973000	4.327685000	4.576289000
C	-4.963321000	1.000810000	-0.555599000
H	-5.639102000	0.515068000	-1.268249000
H	-5.522992000	1.161077000	0.372466000
H	-4.706680000	1.979842000	-0.959825000
C	4.950144000	-0.408050000	-0.743968000
H	5.569183000	-0.429745000	0.159545000
H	5.433000000	-1.049123000	-1.489720000
H	4.962309000	0.611536000	-1.128661000
C	4.257627000	-4.362974000	0.812702000
H	5.213477000	-4.569847000	1.296678000
H	3.494792000	-4.417557000	1.592573000
C	3.990378000	-5.397650000	-0.284199000
H	4.781874000	-5.375869000	-1.037042000
H	3.036064000	-5.215017000	-0.783268000
H	3.960234000	-6.399059000	0.152829000
C	-5.340738000	-2.994800000	1.004467000

H	-4.596117000	-3.263480000	1.757058000
H	-6.298630000	-2.930907000	1.522914000
C	-5.410487000	-4.056717000	-0.096726000
H	-4.461228000	-4.144307000	-0.630006000
H	-6.190423000	-3.811051000	-0.821316000
H	-5.645110000	-5.029405000	0.343215000
H	-5.842901000	-1.071861000	0.292483000
H	5.247739000	-2.654086000	0.068134000

Urea, C1, imaginary frequency=0, E= -225.364651 a.u

N	-1.160289000	-0.596581000	-0.049250000
O	0.000048000	1.364954000	0.010925000
C	0.000002000	0.131006000	-0.000984000
N	1.160256000	-0.596656000	-0.049307000
H	-2.011279000	-0.093102000	0.145281000
H	2.011227000	-0.093208000	0.145402000
H	-1.164884000	-1.583339000	0.158758000
H	1.164765000	-1.583363000	0.158958000

Thiourea, C1, imaginary frequency=0, E= -548.3200771 a.u

N	1.043467000	-1.145957000	-0.000116000
S	-1.366249000	0.000000000	-0.000020000
C	0.341039000	0.000000000	0.000139000
N	1.043467000	1.145957000	-0.000134000
H	0.549659000	-2.022679000	0.000469000
H	0.549660000	2.022679000	0.000501000
H	2.052950000	-1.165747000	0.000101000
H	2.052950000	1.165747000	0.000172000

Selenourea, C1, imaginary frequency=0, E= -2551.6517451 a.u

N	1.555301000	-1.145933000	0.000299000

Se	-1.006257000	0.000000000	-0.000016000
C	0.865111000	0.000000000	0.000021000
N	1.555301000	1.145933000	0.000289000
H	1.058077000	-2.021183000	-0.000816000
H	1.058078000	2.021183000	-0.000814000
H	2.565845000	-1.172896000	-0.001073000
H	2.565846000	1.172895000	-0.001003000

23. References.

1 K. Mishra, A. Das and S. Ghosh, *J. Phys. Chem. C*, 2020, **124**, 24115-24125.

2 J. R. Lakowicz, *Principles of fluorescence spectroscopy*, Springer science & business media, 2013.

3 A. Pabbathi and A. Samanta, *J. Phys. Chem. B*, 2015, **119**, 11099-11105.

4 M. J. Frisch, G. W. Trucks, H. B. Schlegel, G. E. Scuseria, M. A. Robb, J. R. Cheeseman, G. Scalmani, V. Barone, G. A. Petersson, H. Nakatsuji, X. Li, M. Caricato, A. V. Marenich, J. Bloino, B. G. Janesko, R. Gomperts, B. Mennucci, H. P. Hratchian, J. V. Ortiz, A. F. Izmaylov, J. L. Sonnenberg, Williams, F. Ding, F. Lipparini, F. Egidi, J. Goings, B. Peng, A. Petrone, T. Henderson, D. Ranasinghe, V. G. Zakrzewski, J. Gao, N. Rega, G. Zheng, W. Liang, M. Hada, M. Ehara, K. Toyota, R. Fukuda, J. Hasegawa, M. Ishida, T. Nakajima, Y. Honda, O. Kitao, H. Nakai, T. Vreven, K. Throssell, J. A. Montgomery Jr., J. E. Peralta, F. Ogliaro, M. J. Bearpark, J. J. Heyd, E. N. Brothers, K. N. Kudin, V. N. Staroverov, T. A. Keith, R. Kobayashi, J. Normand, K. Raghavachari, A. P. Rendell, J. C. Burant, S. S. Iyengar, J. Tomasi, M. Cossi, J. M. Millam, M. Klene, C. Adamo, R. Cammi, J. W. Ochterski, R. L. Martin, K. Morokuma, O. Farkas, J. B. Foresman and D. J. Fox, *Journal*, 2016.

5 B. C. Swain, S. K. Mukherjee, J. Rout, Sakshi, P. P. Mishra, M. Mukherjee and U. Tripathy, *Anal. Bioanal. Chem.*, 2020, **412**, 2565-2577.

6 M. M. Islam, S. Barik, N. Preeyanka and M. Sarkar, *J. Phys. Chem. B*, 2020, **124**, 961-973.